

Optical Engineering

OpticalEngineering.SPIEDigitalLibrary.org

Preliminary study on atmospheric-pressure plasma-based chemical dry figuring and finishing of reaction-sintered silicon carbide

Xinmin Shen
Hui Deng
Xiaonan Zhang
Kang Peng
Kazuya Yamamura

Preliminary study on atmospheric-pressure plasma-based chemical dry figuring and finishing of reaction-sintered silicon carbide

Xinmin Shen,^{a,*} Hui Deng,^b Xiaonan Zhang,^a Kang Peng,^a and Kazuya Yamamura^{c,*}

^aPLA University of Science and Technology, College of Field Engineering, Research Center for Mechanical and Electrical Engineering, Haifu Street, Nanjing, Jiangsu 210007, China

^bSingapore Institute of Manufacturing Technology, 71 Nanyang Drive, 638075, Singapore

^cOsaka University, Graduate School of Engineering, Research Center for Ultra-Precision Science and Technology, 2-1 Yamadaoka, Suita, Osaka, 565-0871, Japan

Abstract. Reaction-sintered silicon carbide (RS-SiC) is a research focus in the field of optical manufacturing. Atmospheric-pressure plasma-based chemical dry figuring and finishing, which consist of plasma chemical vaporization machining (PCVM) and plasma-assisted polishing (PAP), were applied to improve material removal rate (MRR) in rapid figuring and ameliorate surface quality in fine finishing. Through observing the processed RS-SiC sample in PCVM by scanning white-light interferometer (SWLI), the calculated peak-MRR and volume-MRR were $0.533 \mu\text{m}/\text{min}$ and $2.78 \times 10^{-3} \text{mm}^3/\text{min}$, respectively. The comparisons of surface roughness and morphology of the RS-SiC samples before and after PCVM were obtained by the scanning electron microscope and atomic force microscope. It could be found that the processed RS-SiC surface was deteriorated with surface roughness rms 382.116nm . The evaluations of surface quality of the processed RS-SiC sample in PAP corresponding to different collocations of autorotation speed and revolution speed were obtained by SWLI measurement. The optimal surface roughness rms of the processed RS-SiC sample in PAP was 2.186nm . There were no subsurface damages, scratches, or residual stresses on the processed sample in PAP. The results indicate that parameters in PAP should be strictly selected, and the optimal parameters can simultaneously obtain high MRR and smooth surface. © The Authors. Published by SPIE under a Creative Commons Attribution 3.0 Unported License. Distribution or reproduction of this work in whole or in part requires full attribution of the original publication, including its DOI. [DOI: 10.1117/1.OE.55.10.105102]

Keywords: optical machining; reaction-sintered silicon carbide; plasma chemical vaporization machining; plasma-assisted polishing; material removal rate; surface quality.

Paper 161174 received Jul. 31, 2016; accepted for publication Sep. 22, 2016; published online Oct. 18, 2016.

1 Introduction

Reaction-sintered silicon carbide (RS-SiC) ceramic is a promising optical material because of its excellent mechanical, chemical, thermal, and electrical properties,^{1,2} which makes it a research focus in the field of optical machining. However, it is difficult to obtain a high material removal rate (MRR) in figuring RS-SiC for its high mechanical hardness and strong chemical inertness.^{3,4} What is more, the fabrication process of RS-SiC generates SiC and Si domains in the RS-SiC substrate, and the asymmetric components make it difficult to obtain a high surface quality in the fine finishing of RS-SiC.^{5,6} Along with the increasing demands of RS-SiC products with high quality, it is urgently required to develop unique processing techniques.

Many techniques have been developed to process this traditional difficult-to-machine material, but few of them can simultaneously obtain high MRR and fine surface quality in machining RS-SiC.⁷ An efficient way is the combination of a rapid figuring method and a fine finishing method. Plasma chemical vaporization machining (PCVM) is a machining method with chemical material removal by the F radical.^{8,9} Owing to the controllable chemical reaction rate, the MRR in PCVM can be enlarged by adjusting the processing

parameters.¹⁰ Plasma-assisted polishing (PAP) includes the oxidation of the substrate by the water vapor plasma and the removal of oxide by the abrasive polishing.¹¹ Due to the hardness differences between the substrate and oxide, PAP can achieve an ultrasurface, which has been verified in machining single crystal 4H-SiC samples.^{12,13} Therefore, the application of atmospheric-pressure plasma-based chemical dry figuring and finishing, which consist of PCVM and PAP, is investigated to verify its feasibility to process RS-SiC in this study.

After PCVM of RS-SiC samples, scanning white-light interferometer (SWLI) measurement was conducted to calculate the MRR and evaluate the surface quality, and the scanning electron microscope (SEM) and the atomic force microscope (AFM) were used to investigate the surface morphology. Meanwhile, PAP was applied to improve the surface quality of the processed RS-SiC sample in PCVM, and the surface roughnesses corresponding to different polishing parameters were obtained by SWLI measurements. By the investigation on MRR in PCVM and the study on surface quality in PAP, the feasibility of these techniques was verified.

2 Experimental Apparatus

The schematic diagram of the PCVM system is shown in Fig. 1(a).^{14,15} The electrode for generating plasma was constructed from coaxially arranged metal electrode and alumina

*Address all correspondence to: Xinmin Shen, E-mail: shenxmjff@gdx2014@163.com; Kazuya Yamamura, E-mail: yamamura@upst.eng.osaka-u.ac.jp

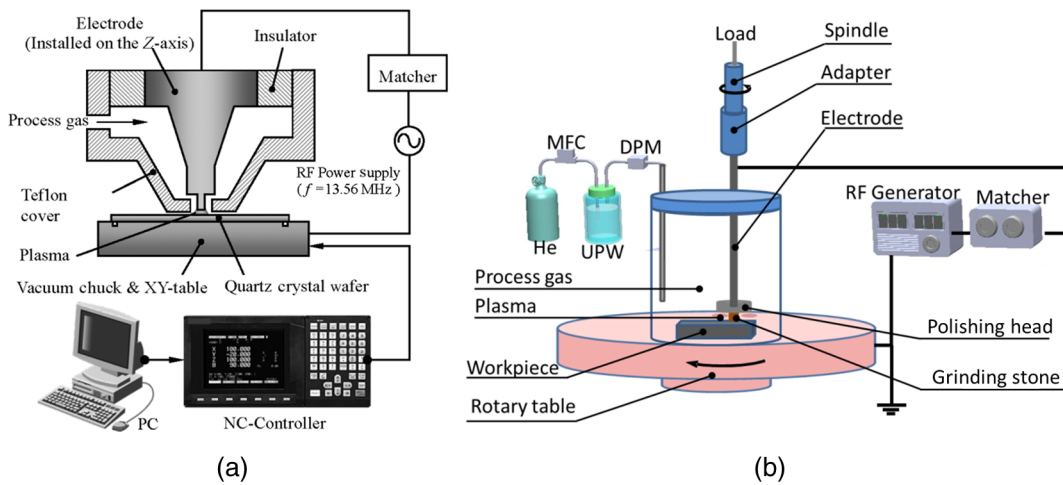


Fig. 1 Schematic diagram of the experimental apparatus: (a) PCVM and (b) PAP systems.

(Al₂O₃) ceramic tube. The diameter and material of the electrode were 3 mm and aluminum (Al) alloy, respectively. The composition and flow rate of the processing gas were controlled by the mass flow controller. Supplying of the gas from the circumference of the tip of the electrode replaced the air to the processing gas and enabled the stable generation of the plasma in the atmospheric-pressure environment. The applied high-frequency electric field ($f = 13.56$ MHz) generated the plasma in the narrow gap between the electrode and the substrate, and the typical gap distance was 500 μm .

The schematic diagram of the PAP system is shown in Fig. 1(b).^{16,17} The compound apparatus consisted of the installed plasma generation part and the mechanical polishing part. Atmospheric-pressure plasma was generated by applying an RF ($f = 13.56$ MHz) electric power, and helium (He)-based water vapor with a flow rate of 1.5 L/min was supplied as the process gas. Water vapor was introduced into the process gas by bubbling the He through ultrapure water, and its concentration was measured by the dew-point meter. The used copper (Cu) electrode was covered with quartz glass to prevent the arc discharge in the generation of dielectric barrier discharge. In the mechanical polishing part, the RS-SiC sample was fixed on the rotary table. The resin

bonded ceria (CeO₂) grinding stone was installed on the polishing head. An insulative adapter was used to connect the spindle and the electrode, which could protect the motor. The load was set to 10 g, which was propitious to obtain high surface quality in the polishing process. First, the RS-SiC sample was processed by PCVM. Afterward, PAP was conducted to finish the surface of the processed RS-SiC sample in PCVM.

3 Results and Discussion

3.1 Reaction-Sintered Silicon Carbide Sample Processed by Plasma Chemical Vaporization Machining

The MRR of RS-SiC in PCVM was obtained by SWLI measurement, as shown in Fig. 2. The RF power, compositions and flow rates of the process gases, and machining time were 100 W, He (750 ml/min), CF₄ (5 ml/min), O₂ (5 ml/min), and 90 s, respectively. It could be calculated that the peak-MRR was 0.533 $\mu\text{m}^3/\text{min}$, and the volume-MRR was 2.78×10^{-3} mm³/min. Relative to the present methods for machining RS-SiC, such as the single-point diamond turning,¹⁸ electrolytic in-process dressing grinding,¹⁹

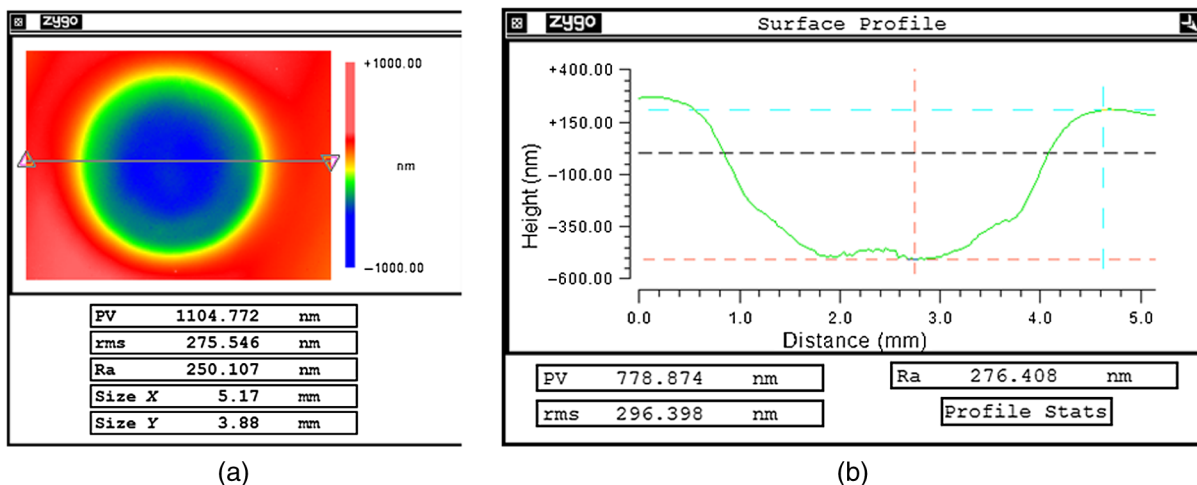


Fig. 2 Calculation of the MRR in PCVM of RS-SiC sample obtained by SWLI measurement: (a) typical shape of the removal spot and (b) cross-sectional line of the removal spot.

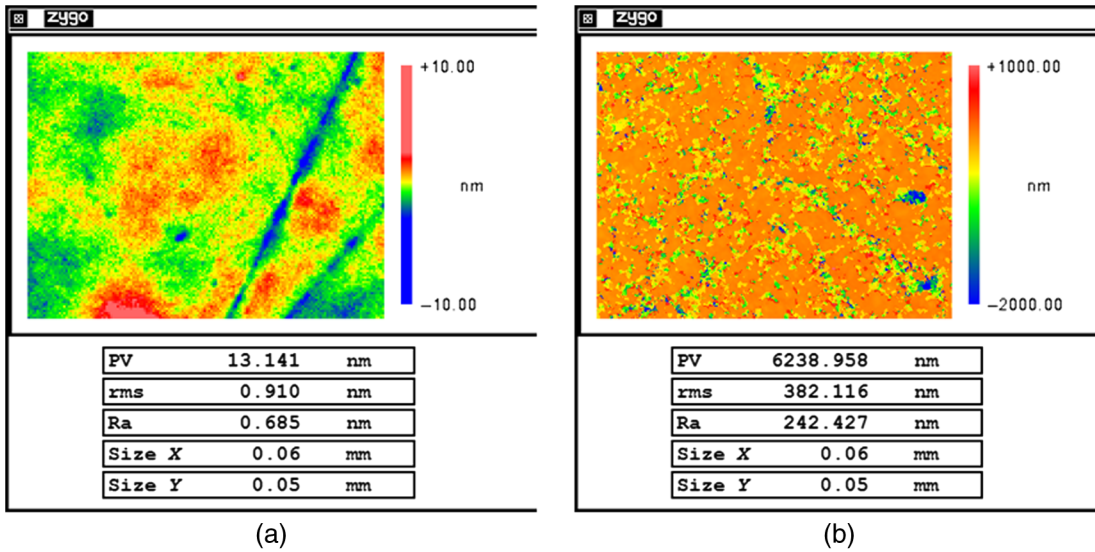
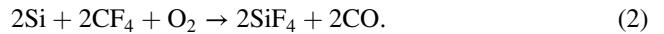


Fig. 3 Comparisons of surface roughness of the RS-SiC sample before and after PCVM: (a) the initial surface obtained by diamond lapping and (b) the processed surface obtained by PCVM.

and magnetorheological finishing,²⁰ the MRR in PCVM of RS-SiC is considerable. What is more, PCVM is a non-contact figuring technique and the material removal is conducted by chemical reaction, so we suppose that there will be no subsurface damage or residual stresses on the processed sample, which are common in the processed RS-SiC sample obtained by the present mechanical material removal methods. Therefore, PCVM can be treated as an efficient rapid figuring method to process RS-SiC.

The comparisons of surface roughness of the RS-SiC sample before and after PCVM are shown in Fig. 3. It can be found that the initial surface, which was obtained by diamond lapping, had a fine surface roughness rms 0.910 nm. However, from Fig. 3(a), it can be found that there were scratches on the surface, because the hardness of the diamond is higher than that of the RS-SiC. Furthermore, there were small holes on the surface as shown in Fig. 3(a), because the hardnesses of SiC and Si grains in the RS-SiC substrate differ, which resulted in a different micro-MRR among the different grains. After PCVM, the RS-SiC surface was deteriorated, and the surface roughness root-mean-square

(rms) and roughness average (Ra) were 382.116 and 242.427 nm, respectively. The major reason for this phenomenon might be that the chemical reactivities of SiC and Si grains differ. The possible chemical reactions that occurred in the PCVM of RS-SiC are as follows:



Therefore, the MRRs in machining SiC/Si grains by F radicals were nonuniform. The results obtained by SWLI indicated that the PCVM could obtain high MRR in processing RS-SiC but the obtained surface quality was rough. Thus, another method is urgently demanded to improve the surface quality of the processed RS-SiC in PCVM, which can form an integrated technique.

The comparisons of the surface morphology of RS-SiC before and after PCVM at the same position were conducted by SEM, as shown in Fig. 4. From Fig. 4(a), it could be found that there were many small scratches and holes on the initial

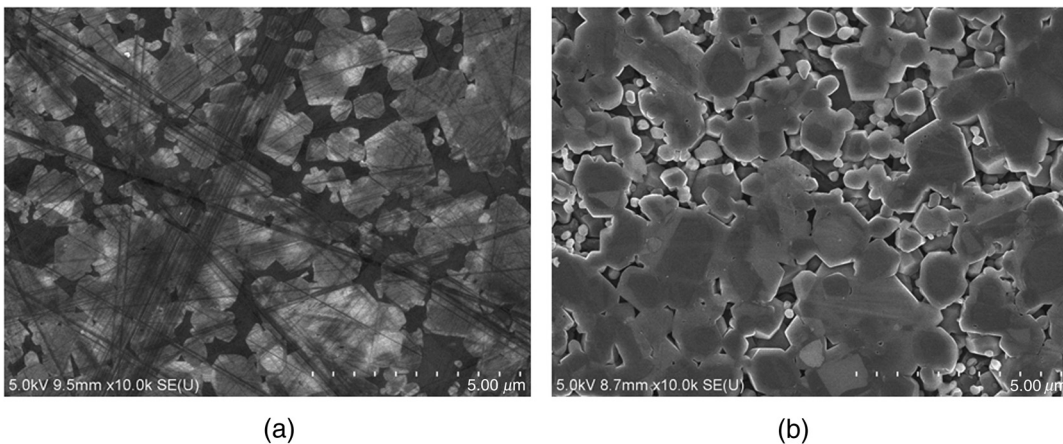


Fig. 4 Comparisons of the surface morphology of RS-SiC sample at the same position obtained by SEM: (a) before and (b) after PCVM.

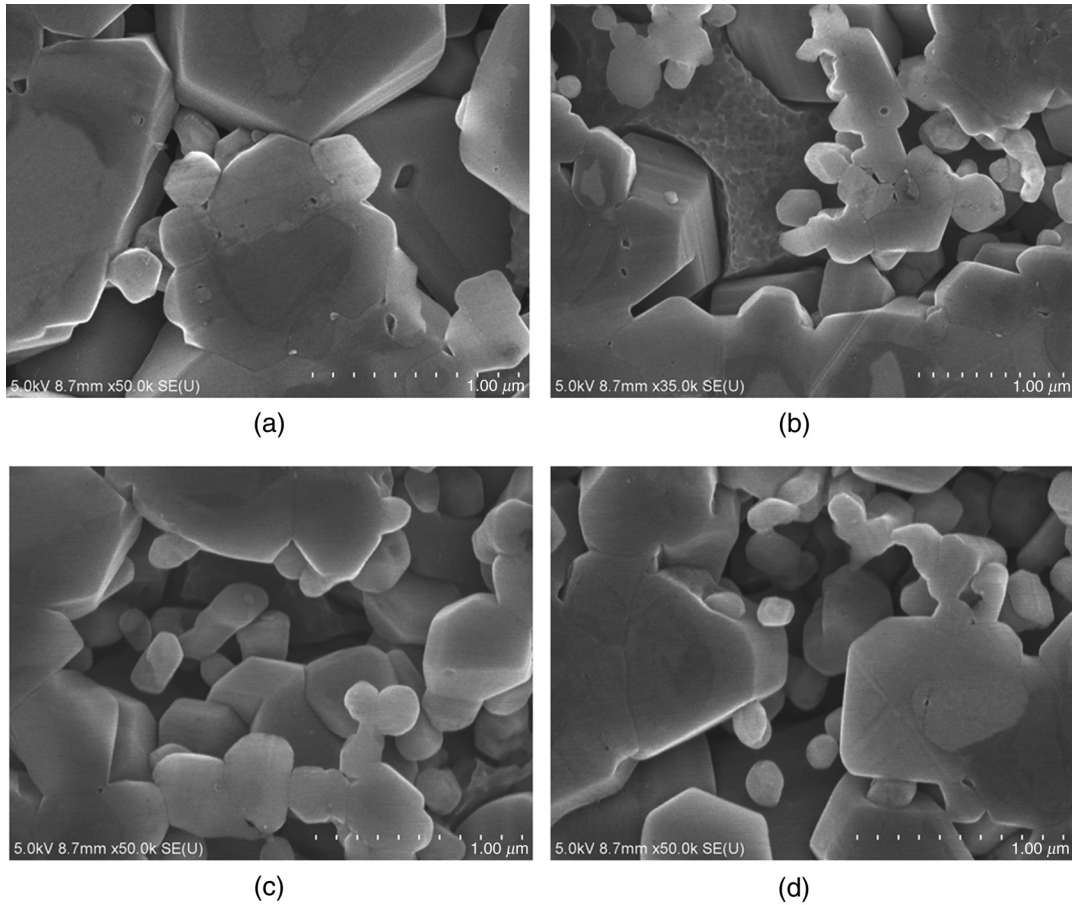


Fig. 5 Details of the processed RS-SiC sample in PCVM obtained by SEM observation under high magnification: (a) the newly exposed SiC grains, (b) the newly revealed Si grains, (c) the shrunken SiC grains, and (d) the weakened connects among different SiC grains.

surface generated by diamond lapping, which was in accordance with the characters exhibited in Fig. 3(a). The surface of the processed RS-SiC sample in PCVM was bumpy, as shown in Fig. 4(b). Irregular holes were formed at the region of initial Si grains, and the areas of initial SiC grains had relatively smooth surfaces. It could be concluded that the micro-MRR of Si grain was larger than that of SiC grain in the RS-SiC substrate. This phenomenon coincided with the fact that the MRR in PCVM of single crystal Si wafer is

larger than that of single crystal SiC wafer under the same experimental parameters.²¹

The details of the processed RS-SiC sample in PCVM are shown in Fig. 5, which were obtained by SEM observation under high magnification. The outlines of the newly exposed SiC grains were very clear in Fig. 5(a), especially for some large grains. Meanwhile, there were obvious boundaries among the newly revealed Si grain and the SiC grains around it, as shown in Fig. 5(b), and the Si grain had the same

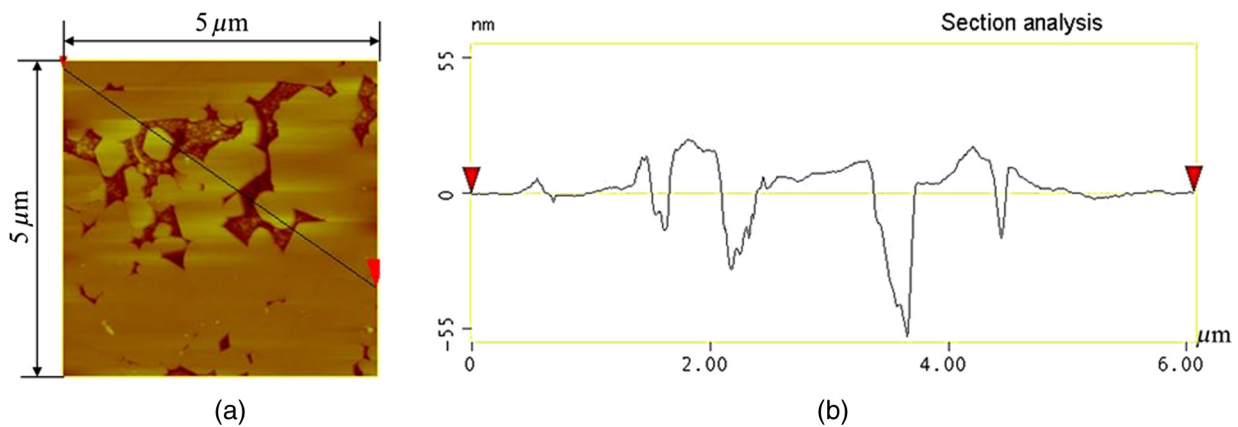


Fig. 6 Quantitative analysis of surface morphology of the processed RS-SiC sample in PCVM by AFM: (a) surface morphology and (b) profile of the cross-sectional line.

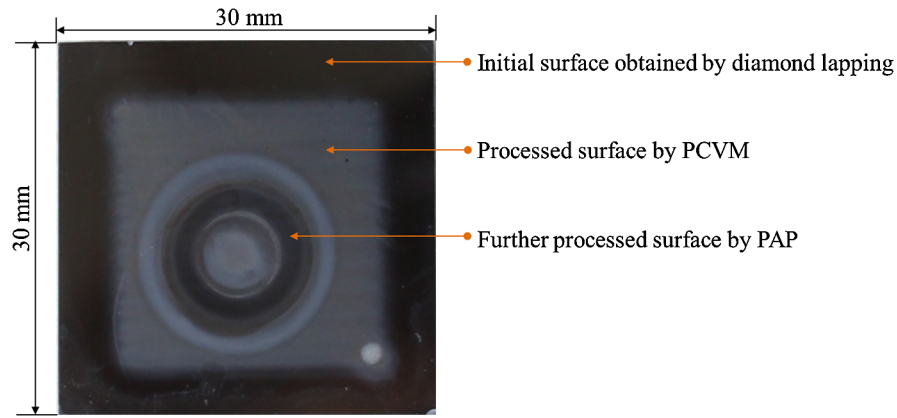


Fig. 7 Illustrations of the initial surface, processed area in PCVM, and processed region in PAP.

characters as the amorphous silicon. What is more, sizes of the SiC grains were shrunken, as shown in Fig. 5(c), because the material removal in PCVM was conducted from the external to the internal on a SiC grain. Furthermore, the connects among different SiC grains were weakened, and there were some almost dissociative SiC grains, as shown in Figs. 5(c) and 5(d), because the chemical reaction rate in the boundary region was larger than that in the central area. Finally, these bumpy structures on the processed RS-SiC could decrease the surface hardness, and the contacting areas between the polishing particle and the abraded sample could be increased. All these features were propitious to

improve the surface quality and the MRR in the further PAP process.

Quantitative analysis of surface morphology of the processed RS-SiC sample in PCVM was obtained by AFM, as shown in Fig. 6. Surfaces of the processed SiC grains in RS-SiC substrate almost remained in a plane, which could be judged from the profile of the cross-sectional line shown in Fig. 6(b). What is more, there were many holes formed at the initial Si regions, and depths of the holes varied from 20 to 60 nm, which further validated the characteristics in PCVM of RS-SiC sample.

Table 1 Experimental parameters in processing RS-SiC by PCVM.

Experimental parameters	Values
RF power supply	100 W
Gap	500 μ m
He + CF ₄ + O ₂	750, 5, 5 ml/min, respectively
Scan mode and scan speed	Raster scan, 200 mm/min
Feed pitch	1 mm

Table 2 The summarized experimental parameters in processing RS-SiC by PAP.

Experimental parameters	Values
RF power supply	32 W
Process gas and its flow rate	He + H ₂ O, 1.5 L/min
Load and pressure	10 g, 10.9 kPa
Grinding stone and its size	Ceria (CeO ₂), square (3 mm × 3 mm)
Polishing head and its size	Aluminum (Al), round (Φ 12 mm)
Eccentricity	9 mm
Polishing time	40 min

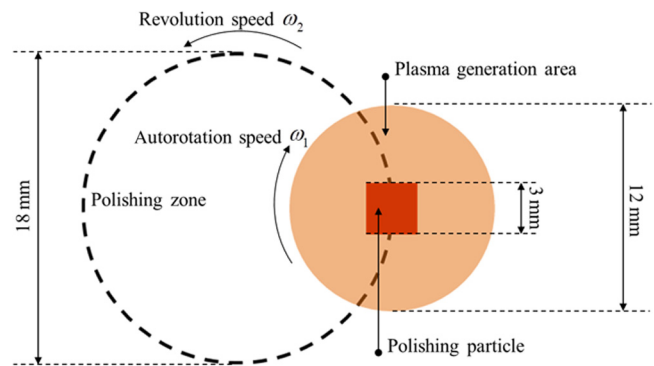


Fig. 8 Schematic diagram of the PAP process with the parameters corresponding to Table 2.

Table 3 The summarized collocations of autorotation speed and revolution speed in PAP.

ω_1	ω_2				
	75 rpm	234 rpm	386 rpm	544 rpm	715 rpm
70 rpm	Group 1	—	Group 7	—	—
100 rpm	Group 2	Group 4	—	—	—
130 rpm	—	Group 5	—	Group 9	—
160 rpm	—	Group 6	—	—	Group 11
200 rpm	Group 3	—	Group 8	Group 10	—

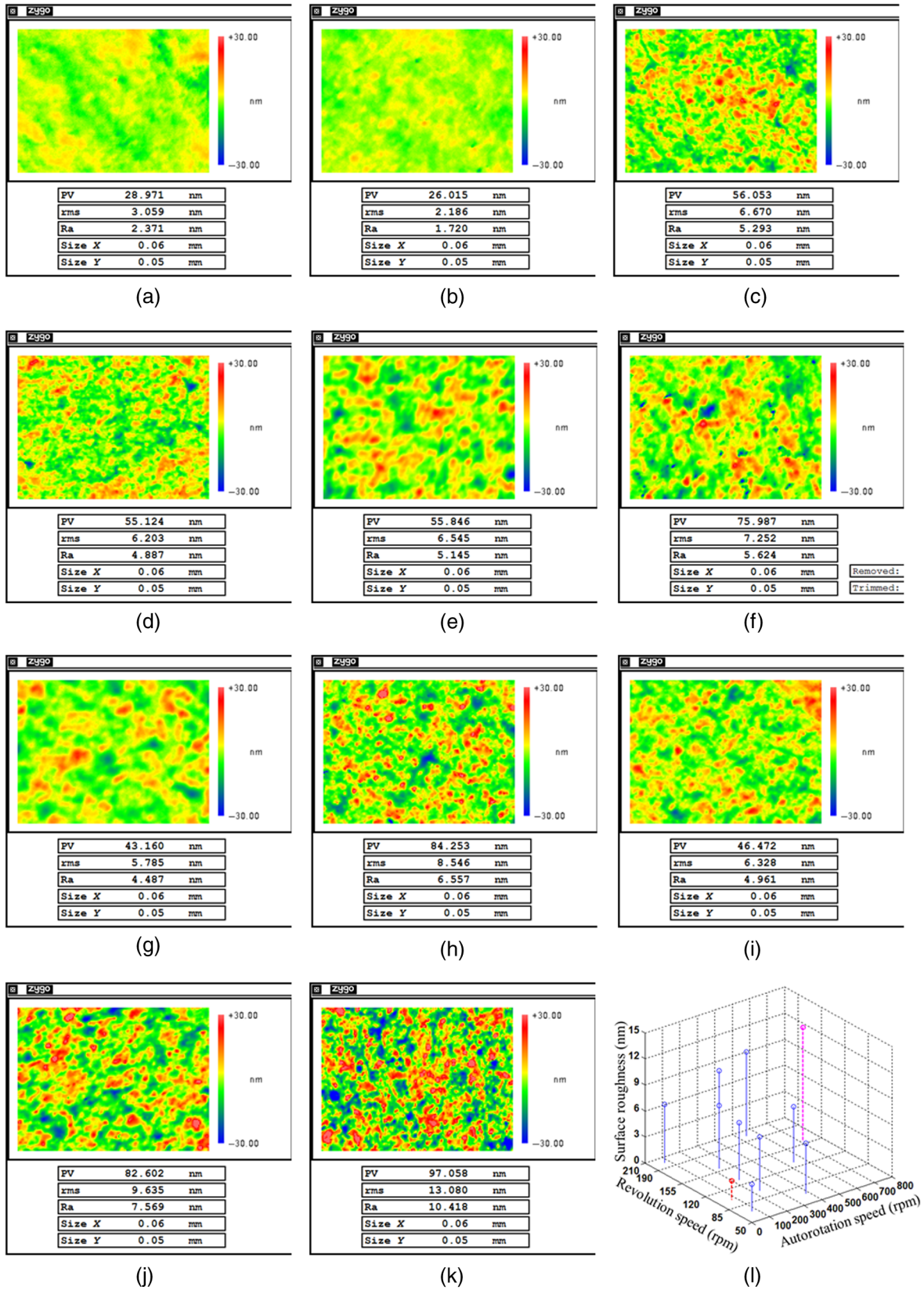


Fig. 9 Evaluations of surface qualities of the processed RS-SiC in PAP corresponding to the different groups: (a) $\omega_1 = 70$ and $\omega_2 = 75$, (b) $\omega_1 = 100$ and $\omega_2 = 75$, (c) $\omega_1 = 200$ and $\omega_2 = 75$, (d) $\omega_1 = 100$ and $\omega_2 = 234$, (e) $\omega_1 = 130$ and $\omega_2 = 234$, (f) $\omega_1 = 160$ and $\omega_2 = 234$, (g) $\omega_1 = 70$ and $\omega_2 = 386$, (h) $\omega_1 = 200$ and $\omega_2 = 386$, (i) $\omega_1 = 130$ and $\omega_2 = 544$, (j) $\omega_1 = 200$ and $\omega_2 = 544$, (k) $\omega_1 = 160$ and $\omega_2 = 715$, and (l) the summarized data.

From research on the MRR, surface quality, and surface morphology of the processed RS-SiC sample in PCVM, it could be concluded that PCVM could be treated as an efficient method for the rapid figuring of RS-SiC, and the surface quality should be further improved.

3.2 Reaction-Sintered Silicon Carbide Sample Processed by Plasma-Assisted Polishing

The PCVM processed RS-SiC sample was further processed by PAP to improve the surface quality. The investigated RS-SiC sample was shown in Fig. 7. The process parameters in PCVM were summarized in Table 1. The size of the RS-SiC sample was 30 mm × 30 mm. The size of the processed area in PCVM was 20 mm × 20 mm, which was realized by controlling the apparatus in Fig. 1(a) in the raster scanning mode with the scan speed of 200 mm/min and feed pitch of 1 mm.

The parameters in processing RS-SiC by the PAP were summarized in Table 2. The schematic diagram of the PAP process was shown in Fig. 8. The autorotation speed ω_1 and revolution speed ω_2 were adjusted to compare the machining results when other parameters were confirmed.

The generation rate of the oxide layer was established when the RF power, process gases, and their flow rates were confirmed. The MRR of the oxide layer could be controlled by adjusting the autorotation speed and revolution speed when the type of grinding stone (polishing particle) and its size, polishing head and its size, and eccentricity were assigned. In the experimental apparatus of PAP as shown in Fig. 1(b), there were five levels for both the autorotation motor and the revolution motor. The selected experiments were organized in 11 groups corresponding to the different collocations of autorotation speed and revolution speed, as shown in Table 3, which aimed to seek the optimal processing parameters.

After PAP, the processed RS-SiC samples were observed by SWLI to evaluate the surface roughness, and the results were shown in Fig. 9. For the purpose of conveniently comparing the surface quality, the obtained surface roughness rms in Fig. 9 was summarized in Table 4. It could be found that the optimal collocation was group 2 (corresponding to $\omega_1 = 100$ and $\omega_2 = 75$), in which the obtained surface roughness rms was 2.186 nm, as shown in Fig. 9(b). Meanwhile, the worst result appeared in the group 11 (corresponding to $\omega_1 = 160$ and $\omega_2 = 715$), in which the achieved surface roughness rms was 13.080 nm, as shown in Fig. 9(k). The experimental results indicated that surface

quality of the processed RS-SiC in PAP was obviously better than that of the surface obtained by PCVM [Fig. 3(b)] and slightly worse than that of the surface obtained by diamond lapping [Fig. 3(a)]. Meanwhile, there were no visible subsurface damages or scratches on the processed sample in PAP, because the hardness of the ceria abrasive grain was smaller than that of the RS-SiC substrate and almost equal to that of the oxide layer. Relative to the obtained ultrasmooth surface (roughness rms 0.629 nm) in the divided PAP (D-PAP) process,⁵ the achieved surface quality in the simultaneous PAP (S-PAP) could be improved by optimizing the process parameters. Meanwhile, the rate in plasma oxidation of RS-SiC was low and the oxide layer prevented the former oxidation of subsurface layer. What is more, in D-PAP, the oxidation and the polishing processes were divided, which indicated that the MRR in D-PAP was obviously smaller than that in S-PAP. Therefore, S-PAP was more suitable for the fine finishing of the RS-SiC sample.

The surface quality of the processed RS-SiC sample in PAP was determined by matching the MRR of oxide layer v_1 with its generation rate v_2 . In this study, the plasma oxidation rate v_2 of the RS-SiC sample was confirmed by the experimental parameters listed in Table 2, and the MRR of the oxide layer v_1 could be controlled by adjusting the autorotation speed ω_1 and the revolution speed ω_2 . Although the actual values of v_1 and v_2 are difficult to obtain, they could be confirmed under certain experimental conditions. If $v_1 = v_2$, the generation of oxide layer entirely matched its removal, which could obtain a relatively smooth surface roughness, as shown in Fig. 9(b), and the PAP of RS-SiC could simultaneously obtain a high MRR and smooth surface in this condition. When $v_1 < v_2$, the oxide layer could not be removed completely and the polishing process was equal to the polished silica (SiO₂) component by ceria abrasion, which was difficult to obtain an ultrasmooth surface, as shown in Fig. 9(a). Otherwise if $v_1 > v_2$, after removal of the oxide layer, the ceria abrasive continued to polish the RS-SiC substrate. The ceria abrasive was seriously abraded, because the hardness of the ceria abrasive grain was distinctly smaller than that of the RS-SiC. The wear degree of the ceria abrasive grain was aggravated along with the increasing of ω_1 and ω_2 , which resulted in a worse surface quality of the processed RS-SiC sample in PAP, as shown in Figs. 9(c)–9(k). The experimental results indicated that parameters in PAP of RS-SiC should be strictly selected, and the optimal parameters simultaneously could obtain high MRR and smooth surface.

4 Conclusions

The combination of PCVM and PAP was conducted to verify the feasibility of these techniques for processing an RS-SiC substrate, which was aimed to improve the MRR in rapid figuring and ameliorate the surface quality in fine finishing. The following conclusions were obtained in this study:

1. Through observation of the processed RS-SiC sample in PCVM by SWLI, the calculated peak-MRR and volume-MRR were 0.533 $\mu\text{m}/\text{min}$ and $2.78 \times 10^{-3} \text{ mm}^3/\text{min}$, respectively. Relative to the conventional techniques for machining RS-SiC sample, the MRR of RS-SiC in PCVM was considerable. Meanwhile, there were no visible subsurface damages, tiny scratches, or residual stresses on the processed

Table 4 The obtained surface roughness rms of the polished RS-SiC sample in each group.

ω_1	ω_2				
	75 rpm	234 rpm	386 rpm	544 rpm	715 rpm
70 rpm	3.059 nm	—	5.785 nm	—	—
100 rpm	2.186 nm	6.203 nm	—	—	—
130 rpm	—	6.545 nm	—	6.328 nm	—
160 rpm	—	7.246 nm	—	—	13.080 nm
200 rpm	6.670 nm	—	8.546 nm	9.635 nm	—

RS-SiC sample because of the noncontact chemical material removal mechanism in PCVM. The results proved that PCVM could be treated as an efficient rapid figuring technique for RS-SiC products.

- By comparing surface roughnesses and morphologies of the RS-SiC samples before and after PCVM, it could be concluded that the processed RS-SiC surface was deteriorated with surface roughness rms 382.116 nm, and the major reason was that the micro-MRR of Si grain was larger than that of the SiC grain. Although the surface of the processed RS-SiC in PCVM was rough, the decrease of hardness and increase of contacting area were propitious in improving MRR in further polishing.
- Evaluations of surface qualities of the processed RS-SiC samples in PAP corresponding to different collocations of autorotation speed and revolution speed were conducted. The optimal surface roughness rms of the PAP processed RS-SiC was 2.186 nm, which was obviously better than that of the surface obtained by PCVM and slightly worse than that of the surface obtained by diamond lapping. What is more, there were no subsurface damages, scratches, or residual stresses on the processed sample, because hardness of the ceria abrasive grain was smaller than that of the RS-SiC and almost equal to that of the oxide.
- Surface quality of the processed RS-SiC in PAP was determined by matching MRR of the oxide with its generation rate. There existed three possibilities: insufficient polishing, optimal polishing, and over polishing. The results indicated that parameters in PAP should be strictly selected, and the optimal parameters could simultaneously obtain high MRR and smooth surface.

The combination of PCVM and PAP can be treated as a technique for RS-SiC, which can improve the machining level of RS-SiC samples and promote the application of RS-SiC products.

Acknowledgments

This work was supported by a grant from the National Key Research and Development Program (Grant No. 2016YFC0802903), a grant from the National Natural Science Foundation of China (Grant No. 51505498), and a grant from the Natural Science Foundation of Jiangsu Province (Grant No. BK20150714). The authors also express their gratitude to the staffs and students of the Research Center for Ultra-Precision Science and Technology, Osaka University.

References

- Z. R. Huang et al., "Manufacture of large-scale lightweight SiC mirror for space," *Proc. SPIE* **8335**, 83351R (2012).

- J. S. Johnson, K. Growsky, and D. J. Bray, "Rapid fabrication of lightweight silicon carbide mirrors," *Proc. SPIE* **4771**, 243–253 (2002).
- S. P. Lee et al., "Fabrication of liquid phase sintered SiC materials and their characterization," *Fusion Eng. Des.* **81**(8–14), 963–967 (2006).
- S. Suyama, T. Kameda, and Y. Itoh, "Development of high-strength reaction-sintered silicon carbide," *Diamond Relat. Mater.* **12**(3–7), 1201–1204 (2003).
- X. M. Shen et al., "Mechanism analysis on finishing of reaction-sintered silicon carbide by combination of water vapor plasma oxidation and ceria slurry polishing," *Opt. Eng.* **54**(5), 055106 (2015).
- Q. Z. Tu et al., "Efficient processing of reaction-sintered silicon carbide by anodically oxidation-assisted polishing," *Opt. Eng.* **54**(10), 105113 (2015).
- J. W. Yan, Z. Y. Zhang, and T. Kuriyagawa, "Mechanism for material removal in diamond turning of reaction-bonded silicon carbide," *Int. J. Mach. Tools Manuf.* **49**(5), 366–374 (2009).
- K. Yamamura, S. Shimada, and Y. Mori, "Damage-free improvement of thickness uniformity of quartz crystal wafer by plasma chemical vaporization machining," *CIRP Ann.—Manuf. Technol.* **57**(1), 567–570 (2008).
- Y. Takeda et al., "Open-air type plasma chemical vaporization machining by applying pulse-width modulation control," *J. Phys. D Appl. Phys.* **47**(11), 115503 (2014).
- H. Takino et al., "Shape correction of optical surfaces using plasma chemical vaporization machining with a hemispherical tip electrode," *Appl. Opt.* **51**(3), 401–407 (2012).
- K. Yamamura et al., "Plasma assisted polishing of single crystal SiC for obtaining atomically flat strain-free surface," *CIRP Ann. Manuf. Technol.* **60**, 571–574 (2011).
- H. Deng et al., "Damage-free dry polishing of 4H-SiC combined with atmospheric-pressure water vapor plasma oxidation," *Jpn. J. Appl. Phys.* **50**(8), 08JG05 (2011).
- K. Yamamura et al., "High-integrity finishing of 4H-SiC (0001) by plasma-assisted polishing," *Adv. Mater. Res.* **126–128**, 423–428 (2010).
- Y. Mori, K. Yamamura, and Y. Sano, "Thinning of silicon-on-insulator wafers by numerically controlled plasma chemical vaporization machining," *Rev. Sci. Instrum.* **75**(4), 942–946 (2004).
- Y. Mori, K. Yamamura, and Y. Sano, "The study of fabrication of the x-ray mirror by numerically controlled plasma chemical vaporization machining: development of the machine for the x-ray mirror fabrication," *Rev. Sci. Instrum.* **71**(12), 4620–4626 (2000).
- H. Deng, M. Ueda, and K. Yamamura, "Chemical and morphological analysis of 4H-SiC surface processed by plasma assisted polishing," *Key Eng. Mater.* **516**, 186–191 (2012).
- H. Deng and K. Yamamura, "XTEM observation of 4H-SiC (0001) surfaces processed by plasma assisted polishing," *Adv. Mater. Res.* **497**, 156–159 (2012).
- H. Y. Tam, H. B. Cheng, and Y. W. Wang, "Removal rate and surface roughness in the lapping and polishing of RB-SiC optical components," *J. Mater. Process. Technol.* **192–193**, 276–280 (2007).
- H. Katahira and H. Ohmori, "ELID grinding characteristics and surface analysis for micro fabrication of advanced ceramics," *Key Eng. Mater.* **339**, 483–489 (2007).
- H. Zhu et al., "Rapid fabrication of lightweight SiC mirror using CCOS," *Proc. SPIE* **8194**, 81942A (2011).
- K. Yamamura, Y. Yamamoto, and H. Deng, "Preliminary study on chemical figuring and finishing of sintered sic substrate using atmospheric pressure plasma," *Procedia CIRP* **3**, 335–339 (2012).

Xinmin Shen received his BS, MS, and PhD degrees in mechanical engineering from the National University of Defense Technology in 2008, 2010, and 2014, respectively. He is a lecturer at the PLA University of Science and Technology. From 2011 to 2013, he studied in Osaka University as a special research student. He is the author of more than 20 papers. His current research focuses on the ultraprecision machining of optical components.

Kazuya Yamamura received his PhD in engineering from Osaka University in 2001. He is an associate professor at Osaka University. His research area is development of unconventional ultraprecision manufacturing process and its application, such as figuring, finishing, functionalization, utilizing reactive plasma, or electrochemical process.

Biographies for the other authors are not available.